

Physics-Informed Neural Networks for Non-linear System Identification applied to Power System Dynamics

Jochen Stiasny, George S. Misyris and Spyros Chatzivasileiadis

Abstract— Varying power-infeed from converter-based generation units introduces great uncertainty on system parameters such as inertia and damping. As a consequence, system operators face increasing challenges in performing dynamic security assessment and taking real-time control actions. Exploiting the widespread deployment of phasor measurement units (PMUs) and aiming at developing a fast dynamic state and parameter estimation tool, this paper investigates the performance of Physics-Informed Neural Networks (PINN) for discovering the frequency dynamics of future power systems and monitoring the system inertia in real-time. PINNs have the potential to address challenges such as the stronger non-linearities of low-inertia systems, increased measurement noise, and limited availability of data. The estimator is demonstrated in several test cases using a 4-bus system, and compared with state of the art algorithms, such as the Unscented Kalman Filter (UKF), to assess its performance.

I. INTRODUCTION

Dynamic security assessment of power systems heavily relies on the accuracy of system models, as well as the knowledge of system parameters that play a crucial role on the system stability [1]. However, the gradual replacement of synchronous generators with converter-connected devices of varying generation and demand (e.g. solar PV, wind turbines, electric vehicles) leads to (i) faster frequency dynamics with larger frequency deviations, and (ii) substantially higher uncertainty in system parameters, such as inertia and damping, that become difficult to track [2], [3].

Dynamic state estimation in power systems has been designed primarily around the Bayesian approach of an a priori probability distribution function for the system states that are subsequently updated with the likelihood of a measurement to form an a posteriori probability distribution [4]. This leads to the family of filtering methods, such as the Kalman filter and its derivatives, e.g. the unscented Kalman filter. For parameter estimation, the filter not only includes the internal states of the system but is usually augmented with the unknown system parameters. These filter-based methods offer the potential for fast implementation which allows for online parameter estimation and state tracking, as well as fault detection. However, the handling of strong non-linearity, and the difficult initialisation due to numerical difficulties constrain the applicability of these methods.

To overcome the challenges of these methods, the use of feed-forward neural networks, primarily for static state estimation, has been proposed in the literature [5], [6]. These

approaches are, however, model agnostic, and especially when it comes to dynamic state estimation of time-varying systems they do not address two main challenges. First, the underlying parameters are unknown. As a result, we are dealing by design with an unsupervised learning problem, as there does not exist a known desired outcome to train against. Second, reliable, structured and extensive data sets are often not available. These two fundamental obstacles have been recently addressed by physics-informed neural networks, which can incorporate the underlying physical laws that the dynamic system shall comply with in the training procedure [7]. In our previous work, we have developed and applied physics-informed neural networks to accurately determine state variables of power systems dynamics [8]. Neural network training procedures also coupled with some physical models have also been applied for the static state estimation of distribution systems [9].

This paper investigates the application of physics-informed neural networks (PINNs) for non-linear parameter estimation in power system dynamics. The following properties of PINNs make this particularly interesting: PINNs are continuous and differentiable with respect to their input - usually time -, they are able to incorporate non-linear system dynamics, and offer a great flexibility to handle noise as well as incomplete data with small and intelligible adjustments. These qualities set them apart from existing methods which are largely built around linearisation and discretisation of the system dynamics, and usually have a limited range of application.

In this paper we therefore, lay out the fundamentals of the method in the context of non-linear system identification and illustrate for the example of a power system how parameters such as the available data, the data quality and the system characteristics affect the accuracy of the estimates.

II. SYSTEM MODEL & METHODOLOGY

In this section we introduce the dynamic system and how the PINN is built up and trained.

A. Dynamic System Model

We consider a dynamic model for a power system that can be expressed in the form of a Differential Algebraic Equation (DAE) system:

$$\dot{\mathbf{x}} = \mathbf{f}(\mathbf{x}, \mathbf{y}, \mathbf{u}; \boldsymbol{\lambda}) \quad (1)$$

$$\mathbf{0} = \mathbf{g}(\mathbf{x}, \mathbf{y}, \mathbf{u}; \boldsymbol{\lambda}) \quad (2)$$

where $\mathbf{f}(\mathbf{x}, \mathbf{y}, \mathbf{u}; \boldsymbol{\lambda})$ corresponds to the first order non-linear differential equations of the system, and $\mathbf{g}(\mathbf{x}, \mathbf{y}, \mathbf{u}; \boldsymbol{\lambda})$ to the algebraic equations relating the outputs of the system to its state variables and inputs. Vector \mathbf{x} represents the dynamic

This work is supported by the multiDC project funded by Innovation Fund Denmark, Grant No. 6154-00020B.

J. Stiasny, G. Misyris and S. Chatzivasileiadis are with the Center for Electric and Power Engineering in the Department of Electrical Engineering, Technical University of Denmark, Lyngby, Denmark

{jbest, gmisy, spchatz}@elektro.dtu.dk

states, \mathbf{y} the algebraic variables, \mathbf{u} the input variables, and $\boldsymbol{\lambda}$ are the system parameters.

In this paper, we focus on the power system frequency dynamics, which in their simplest and most common form, are described by the swing equation. For each generator k , the resulting system of equations can then be represented by [3], [10]:

$$m_k \ddot{\delta}_k + d_k \dot{\delta}_k + \sum_j B_{kj} V_k V_j \sin(\delta_k - \delta_j) - P_k = 0 \quad (3)$$

where m_k defines the generator inertia constant, d_k represents the damping coefficient, B_{kj} is the $\{k, j\}$ -entry of the bus susceptance matrix, P_k is the mechanical power of the k^{th} generator, V_k, V_j are the voltage magnitudes at buses k, j and δ_k, δ_j represent the voltage angles behind the transient reactance. $\dot{\delta}_k$ is the angular frequency of generator k , often also denoted as ω_k .

For frequency dependent loads, (3) simplifies to:

$$d_k \dot{\delta}_k + \sum_j B_{kj} V_k V_j \sin(\delta_k - \delta_j) - P_k = 0 \quad (4)$$

where usually $P_k < 0$. For brevity, the term $B_{kj} V_k V_j$ will be referred to as connectivity a_{ij} .

In this paper, we seek to determine uncertain parameters, m_k and d_k , and to estimate voltage phase angles δ_k and generator speeds ω_k . For this we use a set of measurements capturing the temporal evolution of a power system. These could be earlier recorded data or currently observed dynamics.

B. State estimator

The core of the method bases on applying PINNs that were proposed in [7] to the task of state and parameter estimation. In a first step, a classical neural network (NN) is trained to estimate states, e.g. voltage phase angles as in [11]. By applying automatic differentiation (AD) on these estimates we can obtain derivatives of the network output with respect to its input. In our case and as shown in Fig. 1, we supply a time input t and the neural network will return the estimate $u_k(t)$ that shall infer $\delta(t)$. Using AD, we can furthermore extract the temporal derivatives $\dot{u}_k := \frac{\partial}{\partial t} u_k(t)$ which should resemble $\omega(t)$ or even higher order derivatives such as $\ddot{u}_k := \frac{\partial^2}{\partial t^2} u_k(t)$.

The used neural network consists of N_L fully-connected layers with $N^{(n)}$ neurons in the n^{th} layer. The output of the m^{th} layer $y_m^{(n)}$ is described by the following relationship:

$$y_m^{(n)} = \sigma \left(W_{ml}^{(n)} y_l^{(n-1)} + b_m^{(n)} \right), \quad n \in \{1, \dots, N_L\}, \quad (5)$$

$$m \in \{1, \dots, N^{(n)}\}, \quad l \in \{1, \dots, N^{(n-1)}\}$$

where $y_l^{(n-1)}$ the output of the previous layer, $W_{ml}^{(n)}$ the weight matrix, $b_m^{(n)}$ the bias vector and $\sigma(\cdot)$ an activation function. The elements of the weight matrices and bias vectors are variable and will be adjusted throughout the training in an optimisation process as will be described in the following. All weight matrices are initialised as proposed in [12] and the bias vectors are initially set to 0. We use the hyperbolic tangent as the activation function σ for all layers but the final layer $y^{(N_L)}$ where we apply the identity

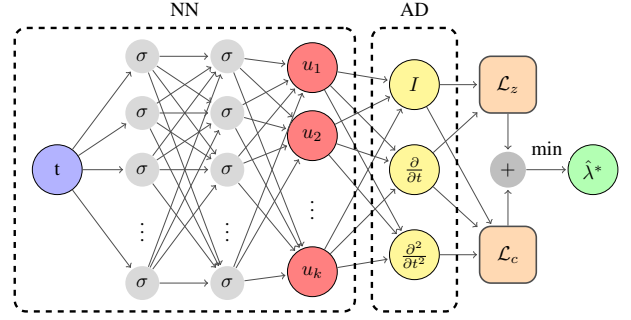


Fig. 1: Physics-informed neural network architecture

function, i.e. no additional non-linearity. For this paper, the neural network input ($y^{(0)}$) is simply the time instance t at which we evaluate the system state. The output ($y^{(N_L)}$) is a vector of the voltage angles estimates $u_k(t)$ of each bus.

By supplying measurements for $\delta_k(t)$ and $\omega_k(t)$, represented as z_k^n and \dot{z}_k^n , we can now train the presented network. We compare the measurements at N_z given instances with the NN's estimates $u_k(t)$ and $\dot{u}_k(t)$ at these points in time. The overall deviation is expressed in the loss function \mathcal{L}_z :

$$\mathcal{L}_z := \frac{1}{N_z} \sum_{n=1}^{N_z} \sum_{k=1}^{N_k} (z_k^n - u_k(t_n))^2 + (\dot{z}_k^n - \dot{u}_k(t_n))^2 \quad (6)$$

C. Physics regularisation

The state estimation presented above falls in the category of supervised learning where we train the network against a desired output: the measurements. However, when the desired output, i.e. the system parameters, is unknown, the problem becomes an unsupervised learning task. In this part of the training, we aim to find parameter estimates \hat{m}_k and \hat{d}_k that yield the best agreement of the underlying physical equations (3) and (4) when checked against the NN output $u_k(t)$ and its temporal derivatives $\dot{u}_k(t)$ and $\ddot{u}_k(t)$. We express this notion in the ‘consistency’ $f_k(t)$ at each bus, effectively applying (3) to the NN outputs:

$$f_k(t) := \hat{m}_k \ddot{u}_k(t) + \hat{d}_k \dot{u}_k(t) + \sum_j a_{kj} \sin(u_k(t) - u_j(t)) - P_k \quad (7)$$

With $f_k(t)$ having to equal 0, so that the NN output will comply with the power system dynamics described by the swing equation, minimizing the regularization term \mathcal{L}_c during training shall lead to neural networks that obey the underlying physical laws of power systems, i.e. physics-informed neural networks:

$$\mathcal{L}_c := \frac{1}{N_c} \sum_{n=1}^{N_c} \sum_{k=1}^{N_k} f_k(t_c)^2 \quad (8)$$

It is important to note that the evaluation of this loss function is not bound to the measured data. Instead it can be evaluated for any time input. We do so by generating N_c equally spaced points across the time domain; we refer to them as collocation points. Furthermore, the value of \mathcal{L}_c can be reduced either by better parameter estimates \hat{m}_k and \hat{d}_k or

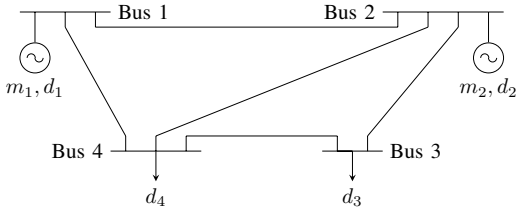


Fig. 2: 4-bus 2-generator system

by a more physically ‘consistent’ estimation for $u_k(t)$, $\dot{u}_k(t)$ and $\ddot{u}_k(t)$. Hence, \mathcal{L}_c also affects the weight matrices and bias vectors of the NN.

D. Training process

By minimising the total loss function $\mathcal{L}_z + \mathcal{L}_c$ over the variables $W_{ml}^{(n)}$, $b_l^{(n)}$, \hat{m}_k and \hat{d}_k , we obtain estimates \hat{m}_k^* and \hat{d}_k^* for the underlying parameters:

$$\hat{m}_k^*, \hat{d}_k^* = \underset{W_{ml}^{(n)}, b_l^{(n)}, \hat{m}_k, \hat{d}_k}{\operatorname{argmin}} \mathcal{L}_z + \mathcal{L}_c \quad (9)$$

However, in practice, (9) poses a highly non-convex and multi-parameter optimisation problem as usually encountered in NN training. We use the Adam optimiser [13], a first-order stochastic gradient-based method, to obtain a solution. The algorithm involves step-wise adjustments of the optimisation variables according to the computed gradient until a sufficiently stable solution is obtained. This requires multiple ‘epochs’, which is simply the number of times the entirety of the available data (collocation points and measurements) has been used in the optimisation. To speed up or even make the training feasible we apply batching of the data points. The batch size is varied during the training, starting with small batches and ending with an optimisation over the whole data set. In practice, this results in initially large adjustments of the parameters to identify the valley of the objective function around the true values such that the final estimation of the parameters can be accurate and is not trapped in another local minimum.

III. SIMULATION

In this section, we briefly introduce the used power system, the training procedure and the unscented Kalman filter, that serves as a comparison.

A. 4-Bus 2-Generator Model

A 4-bus system with two generators as depicted in Fig. 2 is used as a test case. We test three parameter sets, denoted as systems A, B, and C, and shown in I. The three variants shall illustrate how the investigated methods perform in different setups, namely a ‘standard’ system A, a system with faster dynamics (system B), and a system with slower dynamics (system C) compared to the measurement frequency.

Furthermore, we assume to start from an unperturbed state, i.e. $\dot{\mathbf{x}} = 0$ with $\mathbf{u} = 0$ and then add the input signal $\mathbf{u} = \{0.1, 0.2, -0.1, -0.2\} p.u.$ at $t = 0$.

TABLE I: Parameters of the 4-bus 2-generator test case

System Parameters	A	B	C
m_1 (p.u.)	0.3	0.02	5.2
m_2 (p.u.)	0.2	0.03	4.0
d_1 (p.u.)	0.15	0.01	3.8
d_2 (p.u.)	0.3	0.015	4.3
d_3 (p.u.)	0.25	0.02	10.5
d_4 (p.u.)	0.25	0.04	8.3
a_{13} (p.u.)	0.5	0.5	2.5
a_{14} (p.u.)	1.2	1.2	2.2
a_{23} (p.u.)	1.4	1.0	2.0
a_{24} (p.u.)	0.8	0.8	4.8
a_{34} (p.u.)	0.1	0.1	0.7

B. Unscented Kalman Filter

Various nonlinear filters have been used with the Kalman filter framework. Among them, the Unscented Kalman Filter (UKF) has been extensively employed for parameter estimation in power systems [4] and therefore shall serve as a comparison for our method. The UKF is centered around the idea to describe the state \mathbf{x} as a distribution, in this case defined by sigma points. These points are passed through the non-linear function (1), are then weighted, and finally used to form a state prediction together with a covariance and cross-correlation matrix. In the update step, the predictions are combined with the measurements to form the new estimate. A detailed description of the UKF can be found in [14]; here, we follow its notation. In order to estimate m_i^k and d_i^k , we extend the system state $\mathbf{x}^k = [\delta_i^k, \omega_i^k]^T$ by including the unknown parameters $\psi^k = [m_i^k, d_i^k]^T$. The discrete state updates are formulated by discretising (3) and (4).

C. Training procedure

The choice of the NN size plays a key role in how accurately the state predictor can capture non-linearities in the dynamic system. After a thorough investigation, in this paper a PINN with two hidden layers with 30 neurons is chosen, such that all systems can be accurately represented over an input time interval $t \in [0, 2]s$.

Phasor-Measurement-Units (PMUs) allow us to record the voltage angle δ and derive from it the angular frequency $\dot{\delta}$ as specified in the IEEE/IEC International Standard [15]. The sampling frequency for the measurements can range between 10 and 100 frames per second for a 50 Hz system. We simulate measurements every 0.01 seconds, resulting in 200 measurements. We start splitting the data (including 20 collocation points per measurement) in batches of size 200 and then increase them consecutively to $\{400, 800, 2000, 4000\}$ data points. The batches are trained for $\{100, 200, 400, 1000, 4000\}$ epochs respectively. Since the NN’s weights are initialised randomly we run each estimation 20 times. If not mentioned otherwise, these training parameters are applied to each simulation. To test the PINN robustness to noise, as we will see in the next section, we investigate the performance of the methods when we add Gaussian noise with σ up to 5% of the measurement’s value, or a uniform noise distribution of up to $\pm 5\%$.

IV. RESULTS

In this section we want to identify the key features of PINNs by investigating their behaviour in response to

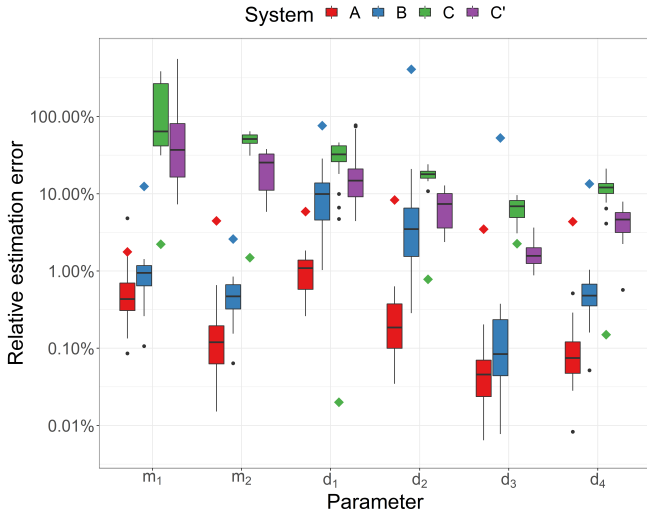


Fig. 3: Accuracy of parameter estimates for PINNs (boxplots) and UKF (diamonds) for the different systems A, B, and C

different systems, input data, and noise.

A. Parameter estimation accuracy

The main objective is to obtain reliable and accurate estimates for the system parameters λ . Fig. 3 shows that PINNs for system A as well as for some parameters in system B achieve a relative error below 1% - performing similarly or better than a UKF. Especially for system B, which is a low-inertia system exhibiting fast dynamics, setting up a UKF proves to be challenging since the ‘high-information’ dynamics occur within only a few time steps which the UKF struggles to capture. Although this also challenges the PINNs, they are still able to estimate a reasonable set of parameters. For slow dynamics, as seen in system C, the UKF recovers the parameters very well in contrast with PINNs. PINNs face the issue that the optimisation landscape is very flat, i.e. no direction of the gradient dominates, and so the adjustment of the weights and parameters in each epoch becomes very small. Eventually, the estimates are either trapped in a local minimum or slowly converge to the underlying parameters. Using a NN with less neurons can partially address this issue as system C’ in Fig. 3 shows.

Investigating the convergence of the two methods, this is best shown as an evolution over epochs for PINNs and an evolution over time for the UKF, as illustrated in Fig. 4. The different x-axes hint at what distinguishes the two methods. The parameter estimates of the UKF, like other filter-based methods, evolve over time as each incoming measurement involves a new filter prediction and update of the parameter estimates. The PINN, in contrast, evolves over epochs, i.e. the number of times the complete data set is used, since each epoch involves a round of optimisation over the loss function and then a (small) update of all variable parameters. Hence, as long as the optimisation is not stuck at a local minimum, additional epochs should drive the estimate closer to the underlying parameters. This repetitive use of the same data set over and over again illustrates a key difference between the two methods: the relation between data points sits at the

core of PINNs in contrast to discrete filters that look at each measurement separately.

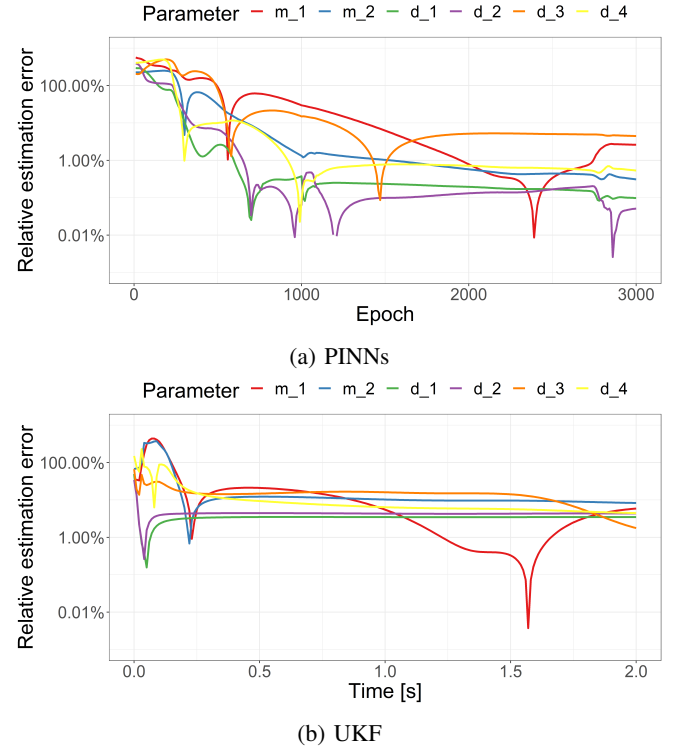


Fig. 4: Evolution of parameter estimates for PINNs and UKF

B. State estimation accuracy

As described in II-B, a part of the PINN functions as a state estimator similar to the state estimates of the UKF. This state estimation initially does not capture the dynamics, however, after a few epochs its estimate matches the true system dynamics very closely as shown in Fig. 5. If we consider the estimated parameters in Fig. 4a at the presented epochs, we note that the parameter estimates show large errors and converge only many epochs later. A central feature of the PINN as a state estimator is that the system state can be directly extracted at any desired time instance

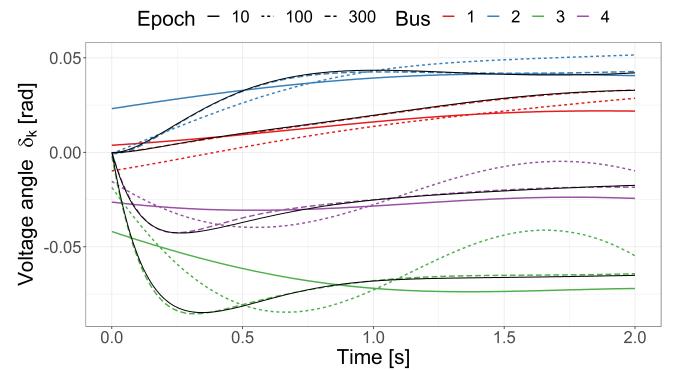


Fig. 5: State estimates of PINN during the training process (black solid lines show the true trajectory).

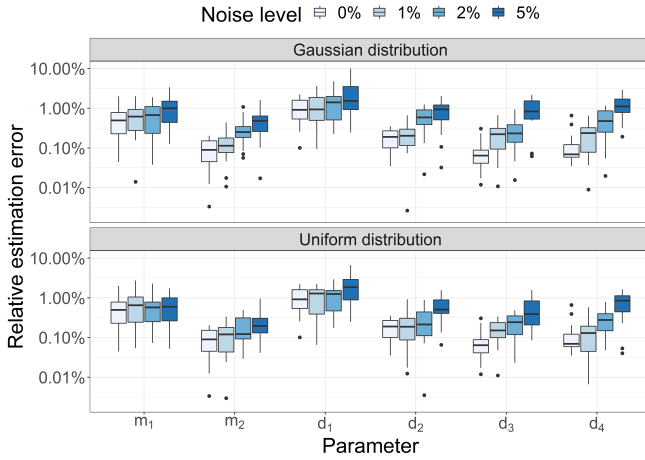


Fig. 6: Parameter estimation accuracy of PINNs for different levels and types of measurement noise

within the time window without the need for interpolation or linearisation of system. This property stems from the continuous and differentiable nature of the PINN and is a fundamental difference compared to the discrete ‘predict-update’ formalism of the UKF. Finally, a key observation related to the PINN’s performance is that the estimator’s nature prevents over-fitting with respect to measurements since the loss \mathcal{L}_c effectively ‘smoothens’ the state estimates. While this is less relevant for measurements with little noise, it becomes important for higher noise levels as it will be shown in the next section.

C. Performance under noise

The robustness to noise has two aspects: how noisy are the measurements and how is the noise distributed. Regarding the noise level, as we would expect, we observe less accurate parameter estimates for increasing noise levels (Fig. 6). Nevertheless, the variation of the parameters remains small across different initialisations of the NN’s weight matrices $W_{ml}^{(n)}$. We furthermore observe that the noise type seems to have a minor impact. This observation and the low impact of noise on the estimate’s accuracy are closely linked to the measurement based loss \mathcal{L}_z since it allows for some deviation of the state estimate from the measurement as long as the deviation remains small. By adapting the loss function \mathcal{L}_z , one could easily incorporate knowledge about the noise to improve the performance and robustness. This once more highlights the great flexibility compared to filter-based methods that are often specifically build around a certain assumption on the noise distribution.

D. Data dependency

A possibly counter-intuitive feature of PINNs is displayed in Fig. 7. We reduce the observed time span from 2 seconds down to 0.2 and 0.5 seconds and hence the number of measurements N_z decreases by a factor of 10 and 4 respectively. The estimation accuracy, though, remains high for parameters apart from d_1 . Furthermore we can observe that the number of collocation points N_c expressed as a multiple of measurement points N_z in Fig. 7 mainly plays a role if few

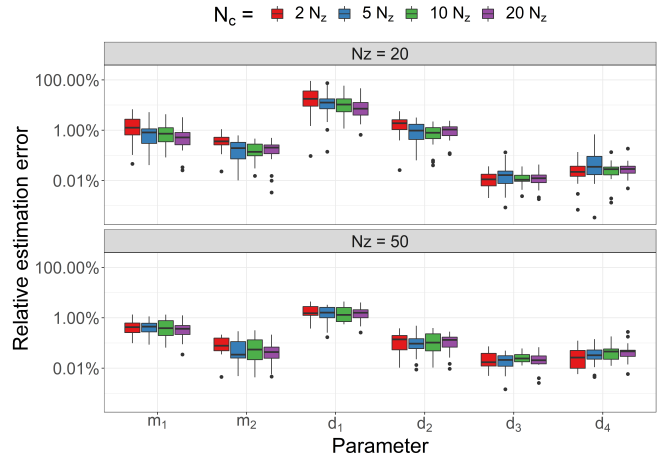


Fig. 7: Parameter estimation accuracy of PINNs for different numbers of measurement and collocation points N_z and N_c .

measurements are available. In these cases, we evaluate the consistency of our estimation with the underlying physics at more points and thereby achieve better estimates. However, the marginal benefit is highest for low ratios N_c/N_z . This is important in the training process since more data points require more time per epoch.

So far we always provided the PINN and the UKF with a complete set of measurements for δ_i and ω_i and only varied the time span and number of collocation points. Let us investigate what happens in the following scenarios where we only use:

- A - (random) 50% of the previous measurements,
- B - measurement of two buses - here bus 1 and 3,
- C - angle measurements, or
- D - frequency measurements.

Fig. 8 reports the results of the various scenarios. The accuracy of the PINN remains similar for scenarios A and D compared to the full data set. In the other two scenarios the parameter estimates are mostly not as accurate, however, the large spread within each estimated parameter suggest that the initialisation and training process affect the estimates. The fact that all these scenarios merely require an adjustment of the training hyper-parameters underlines the great flexibility PINNs can offer to incorporate measurements.

E. Computing time

The flexibility and accuracy of PINNs come at the cost of a computational burden. While an efficient UKF implementation can be executed in real time, the presented PINNs require a training time of up to tens of minutes. This is due to the fact that a NN training is an optimisation in a highly non-convex and high-parameter space, and therefore, it is by design computationally intensive. However, the size of the network (closely related to the system size and the system’s non-linearity), the number of data-points, the batching strategy and the ‘information content’ of the measurements largely influence the required time. By tuning these parameters for each case, as for example for system A, we can train a PINN within 90 seconds.

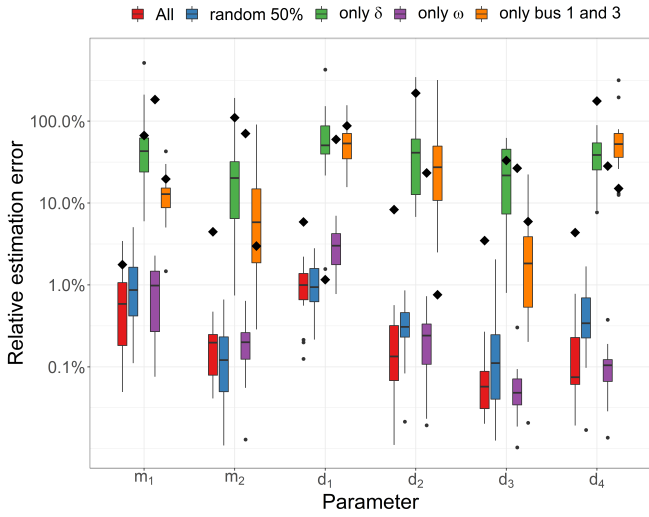


Fig. 8: Estimation accuracy of PINNs (boxplots) and UKF (diamonds) with a subset of measurements. Scenario A has not been implemented for the UKF.

V. DISCUSSION AND OUTLOOK

Physics-informed neural networks can form the basis of a powerful additional tool for dynamic state and parameter estimation. They demonstrate higher accuracy when the system becomes increasingly non-linear, such as during low-inertia periods, are more robust against measurement noise, and perform better if there is limited data availability. However, compared to the Unscented Kalman Filtering method (UKF), PINNs are computationally expensive. Ways to address this issue are to improve the initialisation of the state estimator's weights to achieve faster convergence, and the use of GPUs, code optimisation and additional parallelisation. None of these has been used for the PINNs we trained in this paper.

Having investigated the performance of PINNs and UKF side-by-side in this paper, we expect that hybrid approaches, which use filter-based approaches for the online estimation but rely on PINNs (which have been trained in advance) for the system prediction can achieve the best performance, combining the best of the two methods.

In this paper we focused on estimating the damping and inertia coefficients. However, the same methodology can be applied to estimate system parameters related to nodal voltages and line impedances, i.e. the connectivity $a_{ij} = V_i V_j B_{ij}$, given that it is known which lines are connected, i.e. $B_{ij} \neq 0$. If extended to the context of online monitoring, changes in the system parameters or the system topology could also be detected and identified. An approach in this direction, but based on a different set of methods, has already appeared in the literature [9].

Future work should also investigate the system theoretical aspects of this method, e.g. the observability and stability analysis. Understanding how to interpret PINNs in this context could not only contribute to improve their training procedure but also to build trust into the method which is crucial for applying it in a safety critical context.

VI. CONCLUSIONS

This paper introduced the application of PINNs for dynamic parameter estimation in power systems, and assessed their performance compared to other state-of-the-art dynamic state estimation and system identification methods, such as the Unscented Kalman Filter (UKF). Physics-informed neural networks combine a continuous, differentiable, and non-linear state predictor with a physics regularisation yielding a method which is highly flexible with respect to incorporating measurement data. We have shown that PINNs demonstrate a better performance during periods with stronger nonlinearities, when there is limited availability of measurement data, and against measurements with high noise. Within the discussion of the results, we raised the concern of the higher computational burden, and outlined directions to mitigate it. Future work will focus on the development of hybrid approaches, combining filter-based methods for the online estimation while relying on PINNs for the system prediction, which we expect they will achieve best performance.

REFERENCES

- [1] P. Kundur *et al.*, "Definition and classification of power system stability," *IEEE transactions on Power Systems*, vol. 19, no. 2, 2004.
- [2] F. Milano *et al.*, "Foundations and challenges of low-inertia systems," in *2018 Power Systems Computation Conference*. IEEE, 2018.
- [3] G. S. Misyris, S. Chatzivasileiadis, and T. Weckesser, "Robust frequency control for varying inertia power systems," in *2018 IEEE PES Innovative Smart Grid Technologies Conference Europe*, 2018.
- [4] J. Zhao *et al.*, "Power system dynamic state estimation: Motivations, definitions, methodologies, and future work," *IEEE Transactions on Power Systems*, vol. 34, no. 4, pp. 3188–3198, July 2019.
- [5] K. R. Mestav, J. Luengo-Rozas, and L. Tong, "State estimation for unobservable distribution systems via deep neural networks," in *2018 IEEE Power Energy Society General Meeting (PESGM)*, 2018, pp. 1–5.
- [6] P. N. P. Barbeiro, J. Krstulovic, H. Teixeira, J. Pereira, F. J. Soares, and J. P. Iria, "State estimation in distribution smart grids using autoencoders," in *2014 IEEE 8th International Power Engineering and Optimization Conference (PEOCO2014)*, 2014, pp. 358–363.
- [7] M. Raissi, P. Perdikaris, and G. Karniadakis, "Physics-informed neural networks: A deep learning framework for solving forward and inverse problems involving nonlinear partial differential equations," *Journal of Computational Physics*, vol. 378, pp. 686 – 707, 2019.
- [8] G. S. Misyris, A. Venzke, and S. Chatzivasileiadis, "Physics-informed neural networks for power systems," in *2020 IEEE PES General Meeting (PESGM)*, accepted, 2020. [Online]. Available: <https://arxiv.org/abs/1911.03737>
- [9] L. Zhang, G. Wang, and G. B. Giannakis, "Real-time power system state estimation and forecasting via deep unrolled neural networks," *IEEE Transactions on Signal Processing*, vol. 67, no. 15, pp. 4069–4077, 2019.
- [10] S. Chatzivasileiadis, T. L. Vu, and K. Turitsyn, "Remedial actions to enhance stability of low-inertia systems," in *2016 IEEE PES General Meeting (PESGM)*, 2016, pp. 1–5.
- [11] A. D. Angel, P. Geurts, D. Ernst, M. Glavic, and L. Wehenkel, "Estimation of rotor angles of synchronous machines using artificial neural networks and local PMU-based quantities," *Neurocomputing*, vol. 70, no. 16, pp. 2668 – 2678, 2007.
- [12] X. Glorot and Y. Bengio, "Understanding the difficulty of training deep feedforward neural networks," *Journal of Machine Learning Research - Proceedings Track*, vol. 9, pp. 249–256, 01 2010.
- [13] D. P. Kingma and J. Ba, "Adam: A method for stochastic optimization," 2014.
- [14] M. A. Mohd Ariff, B. Pal, and A. K. Singh, "Estimating dynamic model parameters for adaptive protection and control in power system," *IEEE Transactions on Power Systems*, vol. PP, pp. 1–11, 07 2014.
- [15] "IEEE/IEC International Standard - Measuring relays and protection equipment - Part 118-1: Synchrophasor for power systems - Measurements," *IEC/IEEE 60255-118-1:2018*, pp. 1–78, 2018.